EDGEWOOD

CHEMICAL BIOLOGICAL CENTER

U.S. ARMY RESEARCH, DEVELOPMENT AND ENGINEERING COMMAND

ECBC-CR-095

MASS REMAINING DURING EVAPORATION OF SESSILE DROP

James E. Danberg

SCIENCE APPLICATIONS
INTERNATIONAL CORPORATION
Abingdon, MD 21009

September 2008

Approved for public release;
distribution is unlimited.

ABERDEEN PROVING GROUND, MD 21010-5424

Disclaimer

The findings in this report are not to be construed as an official Department of the Army position unless so designated by other authorizing documents.

REPORT DOCUMENTATION PAGE

Form Approved
OMB No. 0704-0188

1. REPORT DATE *(DD-MM-YYYY)*	2. REPORT TYPE	3. DATES COVERED *(From - To)*
XX-09-2008	Final	May 2006 - May 2007

4. TITLE AND SUBTITLE
Mass Remaining during Evaporation of Sessile Drop

5a. CONTRACT NUMBER
DAAD13-03-D-0017

5b. GRANT NUMBER

5c. PROGRAM ELEMENT NUMBER

6. AUTHOR(S)
Danberg, James E. (SAIC)

5d. PROJECT NUMBER

5e. TASK NUMBER

5f. WORK UNIT NUMBER

7. PERFORMING ORGANIZATION NAME(S) AND ADDRESS(ES)
SAIC, Box 3465A, Box Hill Corporate Drive, Abingdon, MD 21009

8. PERFORMING ORGANIZATION REPORT NUMBER
ECBC-CR-095

9. SPONSORING / MONITORING AGENCY NAME(S) AND ADDRESS(ES)
DIR, ECBC, ATTN: AMSRD-ECB-RT-TD, APG, MD 21010-5424

10. SPONSOR/MONITOR'S ACRONYM(S)

11. SPONSOR/MONITOR'S REPORT NUMBER(S)

12. DISTRIBUTION / AVAILABILITY STATEMENT
Approved for public release; distribution is unlimited.

13. SUPPLEMENTARY NOTES
COTR: Daniel Weber, AMSRD-ECB-RT-TD, (410) 436-2158

14. ABSTRACT-LIMIT 200 WORDS
A theory to predict the evaporation rate of HD (mustard agent) for the special case of a glass substrate has been developed. This is an important reference case for the wind tunnel and field test measurements of the HD evaporation rate. The HD drop is treated as a spherical segment with a constant base diameter characterized by the variation of the droplet shape factor (height to base diameter) or contact angle. A combined variation of diameter and contact angle as a power law function is advanced with the effects of varying the power law exponent investigated. This theory is applied to experimental wind tunnel data; but due to the lack of initial shape factor measurements, appropriate values of shape factor and power law exponents are selected to achieve good agreement. A transformation is introduced that provides an effective method of correlating all the experimental data. The effects of unsteady atmospheric conditions on the mass remaining are due to nonlinearities, and they can be computed by introducing a transformed time.

15. SUBJECT TERMS

HD	Mustard	Mass remaining	Friction velocity
CWA	Schmidt Number	Sherwood Number	Reynolds Number
Contact Angle	Unsteady	Time factor	Transformed time

16. SECURITY CLASSIFICATION OF:			17. LIMITATION OF ABSTRACT	18. NUMBER OF PAGES	19a. NAME OF RESPONSIBLE PERSON
a. REPORT	b. ABSTRACT	c. THIS PAGE			Sandra J. Johnson
U	U	U	UL	33	19b. TELEPHONE NUMBER *(include area code)* (410) 436-2914

Blank

PREFACE

The work described in this report was authorized under Contract No. DAAD13-03-D-0017. The work started in May 2006 and was completed in May 2007.

The use of either trade or manufacturers' names in this report does not constitute an official endorsement of any commercial products. This report may not be cited for purposes of advertisement.

This report has been approved for public release. Registered users should request additional copies from the Defense Technical Information Center; unregistered users should direct such requests to the National Technical Information Service.

Acknowledgments

The author acknowledges the help and encouragement provided by D. J. Weber, Research and Technology Directorate, U.S. Army Edgewood Chemical Biological Center (ECBC), and M. Miller, W. Shuely, R. Nickol, B. King, J. Pence, and C. Franklin, Science Applications International Corporation, Abingdon, MD. D. J. Weber provided overall direction to the project. M. Miller provided drafts of several of the references cited in this report. W. Shuely provided the data on the HD Agent. R. Nickol, B. King, and J. Pence conducted the ECBC experimentation that generated the evaporation data used in this report. C. Franklin is also acknowledged for her assistance in formatting this document for publication.

Blank

CONTENTS

FIGURES

TABLE

MASS REMAINING DURING EVAPORATION OF SESSILE DROP

1. INTRODUCTION

The measurement of the mass remaining is a primary method of experimentally determining the evaporation rate of small drops; therefore, an analytical examination of the problem could be useful. A similar development has been reported by Navez et al.[1] The focus of previous reports[2, 3] in this series has been on the relationship between evaporation rate and the convective environment with the thought that if that were calculated correctly then the problem of the time history of the mass loss would be straightforward, which is only partially correct.

This analysis concerns the special case of drops of a mustard agent, HD, evaporating from a glass substrate. This is an important reference case for the wind tunnel and field test measurements of evaporation rate.

The fundamental relationship involved is

$$\frac{d(\rho_{HD}\forall)}{dt} = -\dot{M} \tag{1}$$

where ρ_{HD} = Mass density of the liquid agent (Kg/m^3)
= 1297.0-1.102*T (°C) for HD*
$\forall$ = Volume of sessile drop (m^3)
$\dot{M}$ = Total drop evaporation rate (Kg/s)
t = Time (s)

If we assume that the sessile drop shape is constant during evaporation and that its configuration is a segment of a sphere, its volume can be described by two variables: the droplet base diameter, d, and a shape factor $\eta = h/d$ (where h = maximum height of the drop), which can also be directly related to the contact angle (β) of the drop, that is $\eta = (1-\cos(\beta))/2\sin(\beta)$.

$$\forall = \frac{\pi}{6} d^3 \left[\frac{3}{4}\eta + \eta^3 \right] \tag{2}$$

* A series of presentations by Him, A. et al.; Navaz, H. et al.; Chakvavarty, S. et al. on "Agent Fate Modeling," Presentation Notes from Agent Fate meeting 14 December 2004.

2. DERIVATION

Since the volume involves two variables, the differentiation requires an assumption regarding their dependence on time. The simplest case occurs when the diameter, d, is a constant and then η is a function of time, which needs to be determined. This is not the only assumption; but, it does form a limiting condition, and it is useful in illustrating the solution technique. It is also tantamount to assuming the droplet height, h, as the unknown.

2.1 Constant Diameter

Equation 1 can now be written as

$$\frac{\pi}{6}d^3\left[\frac{3}{4}+3\eta^2\right]d\eta = -\frac{\dot{M}}{\rho_{HD}}dt \tag{3}$$

Before eq 3 can be integrated, we need to consider the evaporation rate. From the study of the Couette flow problem,[3,4] the evaporation rate can be correlated in terms of the Sherwood (Sh_d), Reynolds (Re_d), and Schmidt (Sc) numbers:

$$\overline{Sh}_d = CSc^{1/3}\,Re_d^{2/3} \tag{4}$$

The definition of the Sh_d number is

$$\overline{Sh}_d = \frac{\dot{M}d}{Ac_wD} \tag{5}$$

where c_w = HD vapor mass concentration at the droplet surface (Kg/m^3)
where it is assumed there is no vapor in the approaching flow.

D = HD diffusion coefficient in air (m^2/s)

A = Droplet evaporating surface area (m^2)

$= \frac{\pi}{4}d^2\left[1+4\eta^2\right]$ note that the term $4\eta^2$ is a correction to the base or plan-form area of the drop to give the full curved surface area.

C = 0.852

The evaporation rate becomes

$$\dot{M} = \frac{\pi}{4}d\left[1+4\eta^2\right]\cdot\left[CSc^{1/3}\,Re_d^{2/3}\right]c_wD \tag{6}$$

A slight simplification can be made at this point by multiplying and dividing by the kinematic viscosity so that we form an inverse Sc number with the D term:

$$\dot{M} = \frac{\pi}{4} d\left[1 + 4\eta^2\right] \cdot \left[CSc^{1/3}\, \mathrm{Re}_d^{2/3} \right] c_w \frac{D}{\nu} \nu = \frac{\pi}{4} d\left[1 + 4\eta^2\right] \cdot \left[C(\mathrm{Re}_d / Sc)^{2/3} \right] c_w \nu \tag{7}$$

Insert eq 7 into eq 3, and eombine η terms and rearrange

$$\frac{4}{6}\left[\frac{\left(\frac{3}{4} + 3\eta^2\right)}{\left(1 + 4\eta^2\right)}\right] d\eta = \left[\mathrm{C(Re_d/Se)^{2/3}} \right] \frac{\mathrm{e_w v}}{\mathrm{d^2 \rho_{HD}}} \mathrm{dt} \tag{8}$$

The left-hand side becomes just $\frac{1}{2} \mathrm{d}\eta$, and because the diameter is a constant, then we ean define a non-dimensional time, ϑ. (This is unneeessary but is eonsistent with putting equations into a non-dimensional form)

$$\vartheta = t \frac{t}{\tau} \tag{9}$$

where we define a time parameter τ with dimensions of seconds

$$\tau = \frac{M_i}{\dot{M}_i} = \frac{2 d^2 \rho_{HD}}{3 c_w C(\mathrm{Re}_d / S_c)^{2/3}} \tag{10}$$

We have taken $\mathrm{M_i} = \frac{\pi}{6} \mathrm{d_i^3 \rho_{HD}}$, and $\dot{M}_i$ is equal to the total droplet initial evaporation rate. (Note the definition of M_i used here is not the initial mass of the droplet beeause the volume used does not aecount for the height of the drop). Now, eq 8 can be written as two simple integrals.

$$\int_{\eta_i}^{\eta} 3 d\eta = -\int_0^{\vartheta} d\vartheta \tag{11}$$

where η_i is the initial value of η at time zero or the start of the droplet evaporation process.

If we assume the $\mathrm{Re_d}$ and Sc numbers remain eonstant as the drop evaporates, the result is

$$3(\eta_i - \eta) = \vartheta \quad \text{or} \quad \eta = \eta_i - \frac{1}{3}\vartheta \tag{12}$$

This result can be put into eq 2 to define the volume as a function of time, or by multiplying with the liquid density, we have the mass remaining as a funetion of time.

Figure 1 shows the result for the following case

Drop = 6 cu-mm
d = 0.0052 m
η_i = 0.1046
T = 35 °C
u_τ = 0.096 m/s
Re_d = 30.3
Sc = 2.53
C = 0.852
ρ_{HD} = 1258. Kg/m^3

Although eq 2 is cubic in the shape factor, there is very little non-linearity in this volume versus time curve. Therefore, it is necessary to include the effect of diameter change as well as shape factor (i.e., droplet height) to correctly simulate the tailing off of the mass remaining as the drop disappears. One way to do this is by switching from shape factor to diameter change at some vague time. This is implied by Navez et al.;[1] but, the implementation is not discussed. In the next section, a suggestion is made on how the two effects can be combined.

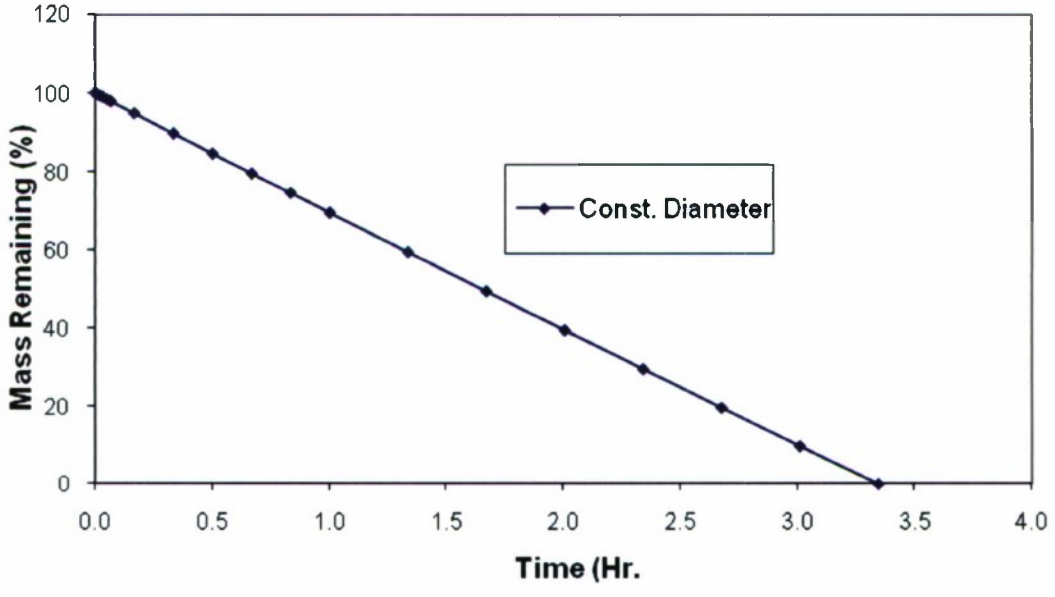

Figure 1. Mass Remaining vs. Time (6 mm^3 Drop, Mid Speed)

2.2 Variable Diameter and Shape Factor

If the diameter d(t) and shape factor $\eta(t)$ are given functions of time, then a solution can be obtained by differentiation of the volume (eqs 1 and 2). But, we could also eliminate time between d and η so that the shape factor becomes a function of diameter

$\eta = f(d)$. One of the simplest relationships is to assume a power law, which can be written in the following form to take care of proportionality factors

$$\frac{\eta(d)}{\eta_i} = \left(\frac{d(t)}{d_i}\right)^m \tag{13}$$

where d_i and η_i are initial values of diameter and shape factor, respectively. The exponent m is analogous to defining the time where the switch is made from constant diameter to constant shape factor. This suggestion is made with the hope that this non-dimensional parameter might have some degree of universality.

To implement the solution with eq 13, a new non-dimensional diameter variable is defined as

$\varphi = \frac{d}{d_i}$ and $\eta = \eta_i \varphi^m$. Equation 2 becomes

$$\forall = \frac{\pi}{6} d_i^3 \left[\frac{3}{4}\eta_i \varphi^{m+3} + \eta_i^3 \varphi^{3m+3}\right] \tag{14}$$

and eq 3 becomes

$$\frac{\pi}{6} d_i^3 \left[\frac{3}{4}\eta_i (m+3)\varphi^{m+2} + \eta_i^3 (3m+3)\eta^{3m+2}\right] d\varphi = -\frac{\dot{M}}{\rho_{HD}} dt \tag{15}$$

Equation 7 is also changed in the following way

$$\dot{M} = \frac{\pi}{4} d_i \varphi^{5/3} \left[1 + 4\eta_i^2 \varphi^{2m}\right] \cdot \left[C(\mathrm{Re}_{di}/Sc)^{2/3}\right] \cdot c_w \nu \tag{16}$$

Remember that d appears to the 5/3 power in the evaporation formula. Also note that the Re_d number is now based on the initial value of the diameter. The combination of eqs 15 and 16 is considerably more complicated, but basically is just algebraic manipulation.

$$\left[\frac{\frac{3}{4}\eta_i (m+3)\varphi^{(3m+1)/3} + \eta_i^3 (3m+3)\varphi^{(9m+1)/3}}{1 + 4\eta_i^2 \varphi^{2m}}\right] d\varphi = -d\vartheta \tag{17}$$

Integration of eq 17 in closed form looks rather formidable. However, eq 17 can be numerically integrated to any desired degree of accuracy for a given value of m.

Numerical integration was performed using a spreadsheet. A number of values of φ were selected, and the left of eq 17 evaluated with mean values of the integrand. Once the relationship between φ and time has been obtained from eq 17, we can go to eq 14 to obtain the volume or mass as a function time.

It is useful to recognize that the denominator in eq 17 for the 6 mm^3 test case is at most, approximately 1.04, and if it is neglected, then eq 17 can be integrated in closed form.

$$\frac{1}{2}\left[\frac{3\eta_i(m+3)}{(3m+4)}(1-\varphi^{(3m+4)/3})+\frac{4\eta_i^3(3m+3)}{(9m+4)}(1-\varphi^{(9m+4)/3})\right]=\vartheta \qquad (18)$$

Figure 2 shows a comparison, for the above conditions, between the numerical integration of eq 17 and the approximate closed form integration of eq 18. They are essentially identical. Figure 2 also shows the constant diameter solution, and it is apparent that the variable diameter solution provides a shape more consistent with what is observed experimentally.

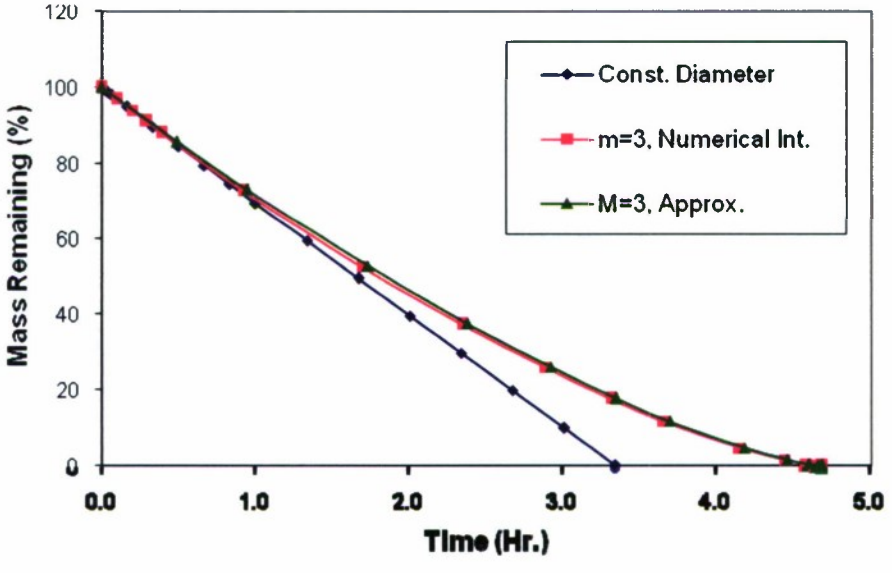

Figure 2. Comparison of the Numerical and Approximate Solution with the Constant Diameter Case

With formulation of this solution technique, we can begin looking at the effect of varying certain parameters such as the exponent m, the choice of initial shape factor, and the Couette correlation constant.

3. EFFECT OF VARYING PARAMETERS

3.1 Exponent m

First, consider varying m the exponent in the relationship between diameter and shape factor.

$$\frac{\eta}{\eta_i} = \left(\frac{d}{d_i}\right)^m \tag{19}$$

It is clear that if m is a large positive number, then η will vary significantly with a rather insignificant change in d. Figure 3 illustrates this with several solutions of eqs 17 and 18 for φ as a function of ϑ. For the m = 5 case, the variation of η/η_i according to eq 19 is also plotted. The η/η_i curve is approaching a linear distribution that corresponds to the constant diameter solution (eq 12).

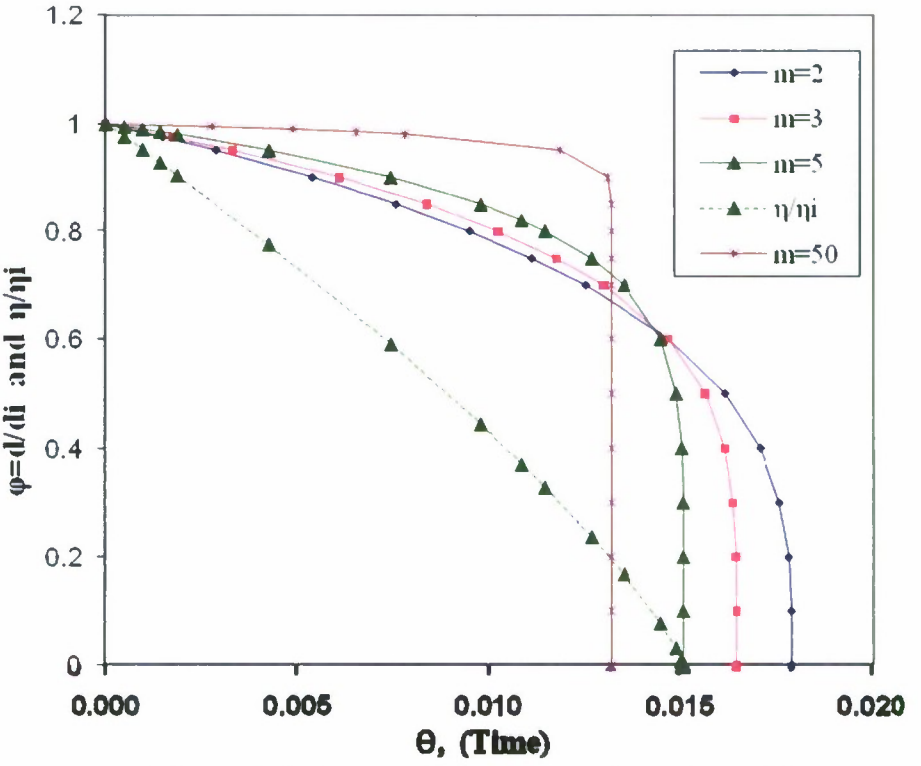

Figure 3. Diameter Parameter as a Function of Time

Note for very high values of m, illustrated by the m = 50 solution, the diameter is essentially constant over the evaporation time except near the end; then, the diameter decreases almost discontinuously. Finally, the total time to evaporate the drop decreases with increasing m with the minimum evaporation time corresponding to $m \to \infty$ or the constant diameter solution.

The mass remaining is shown in Figure 4 as a function of time and the exponent m. The smaller the value of m, the more extended is the tail of the curve and the longer the evaporation time. It is now possible to define the other limiting condition of constant shape factor, which corresponds to m = 0. It is the task of the comparison with experimental data to determine the optimum value of m and to what extent it varies with conditions of the experiments.

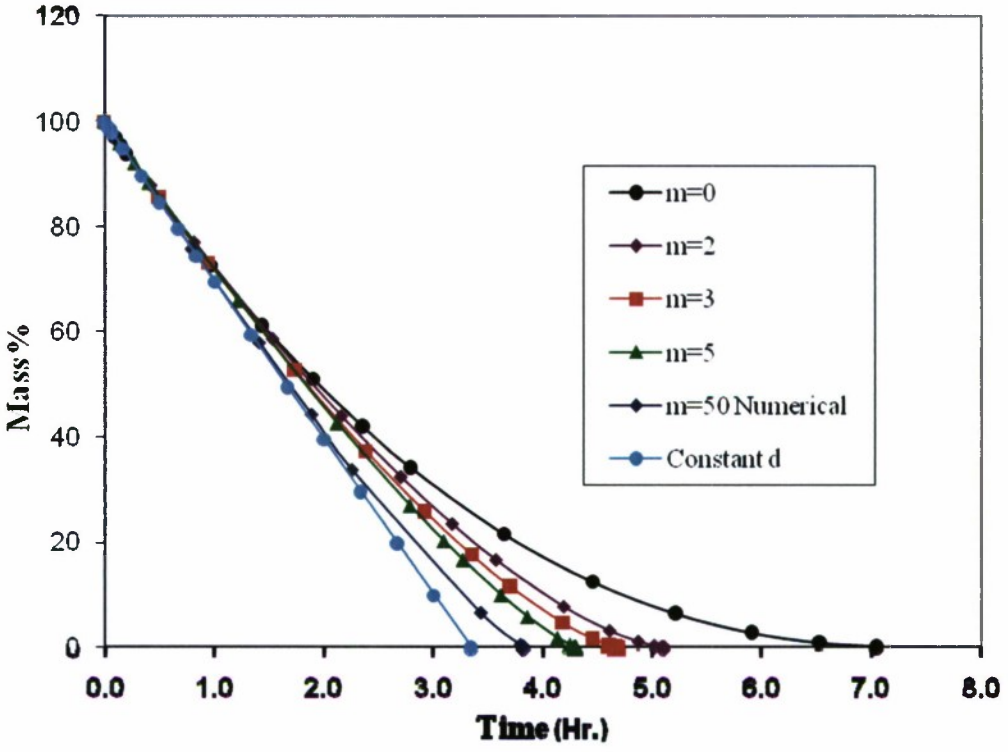

Figure 4. Mass Remaining as a Function of Time and Exponent

Examination of the three 6 mm^3 drops in Figure 3, page 7 of ref 1, it is apparent that the 20% remaining point is somewhere in the 2 - 2.5 hr range, which is less than the value of 2.67 for the constant diameter ($m \rightarrow \infty$) prediction. The discrepancy can not be corrected with m since smaller m values correspond to longer time. For example, at m = 5, the 20% remaining point corresponds to 3.1 hr. There may be some incorrectly calculated experimental conditions that explain the discrepancy. The velocity is specified as wind velocity of 1.77 m/s; but, the friction velocity has been used corresponding to the mid velocity range of the 5-cm tunnel, and that may not be correct. The initial value of the shape factor or contact angle is another quantity that needs to be considered. The average value of 23.6° of the three typical drops (provided by ECBC) has been used here; however, there is a ± 20% difference between them. Ultimately, there is always resort to an ad hoc correction factor in the evaporation rate analysis to improve agreement.

3.2 Contact Angle

Variation of the exponent m is limited by the constant diameter and constant shape factor conditions. It is apparent from the total evaporation times that some results fall

outside these limits. Without modifying the basic model, changing the initial contact angle, β, can either increase or decrease evaporation times significantly. Figure 5 shows the effect on the reference case that we considered. Decreasing β increases the surface area and the evaporation rate considerably. On the other hand, increasing β has a smaller effect on the initial droplet surface area as evidenced by the small change in initial slope; but, large changes in the evaporation time result from the changes in the curvature of the distribution. The m = 0 and m = infinity curves are applicable to the nominal β = 23.6° case and are shown as reference.

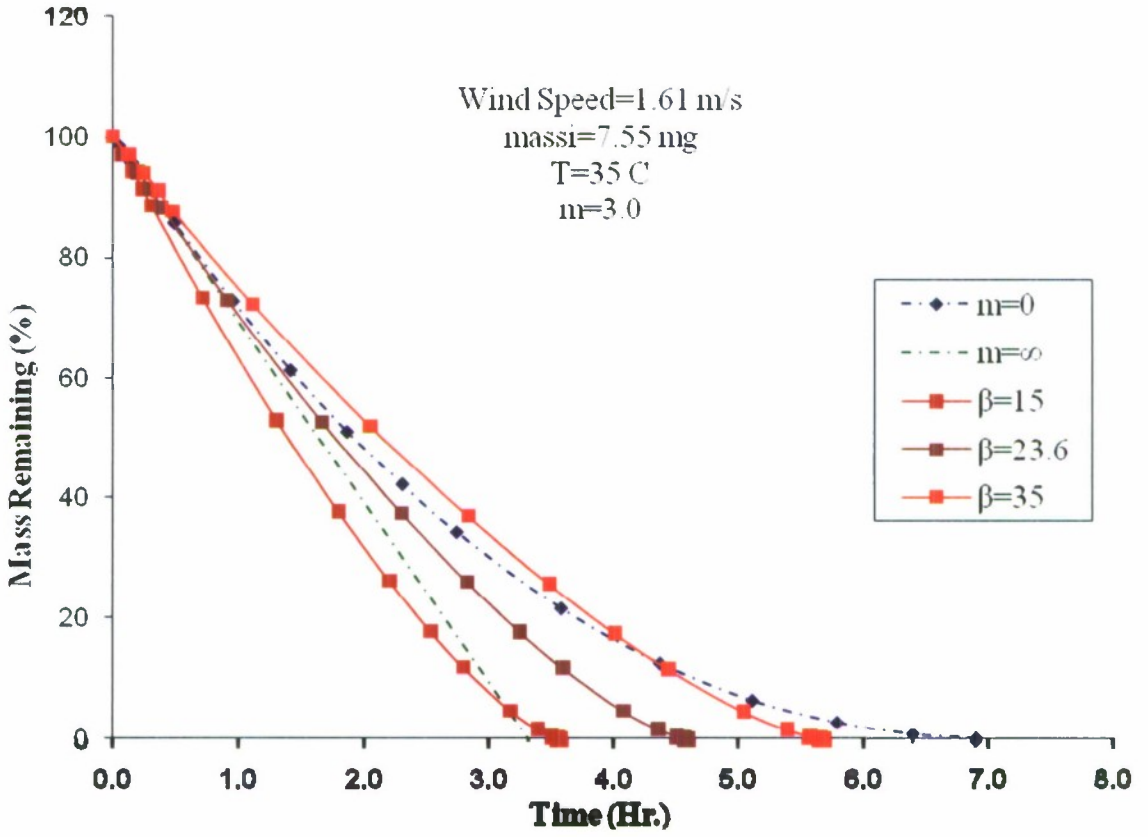

Figure 5. Effect of Varying Initial Contact Angle

In the section comparing the theoretical distribution with experimental data, the analytical curve for a nominal value of the exponent m (say m = 5) is made to agree with the slope or trend of the data by adjusting the contact angle. Adjustments are then made iteratively between m and the β to achieve general agreement although less weight is given to the tail of the experimental distributions because of the inability of the experiment to consistently recover the initial mass of the droplet. This is demonstrated by the experimental data leveling off above and in some cases below the zero mass axes. Figure 6 illustrates this along with a suggested corrected distribution.[5]

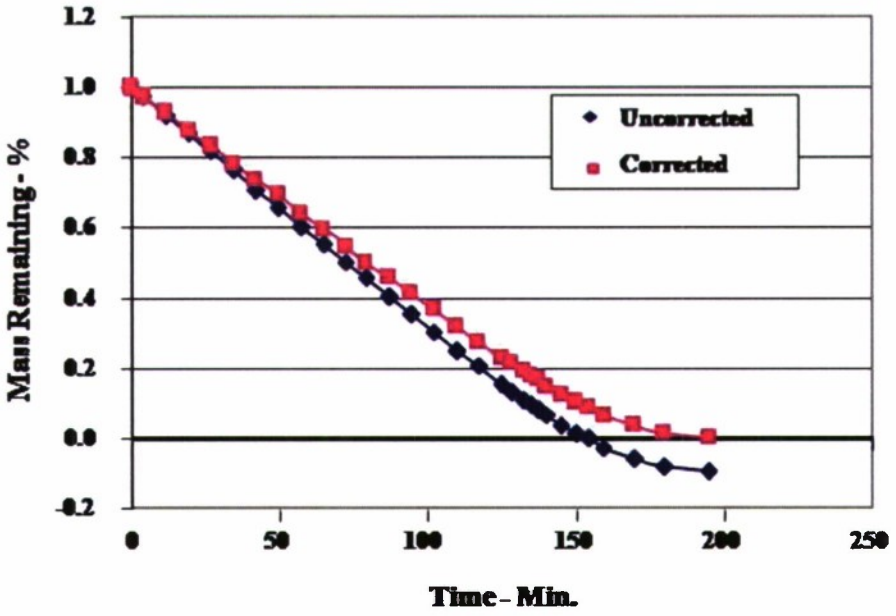

Figure 6. Illustration of Inability in Accounting for the Correct Droplet Mass

4. COMPARISON WITH EXPERIMENTAL DATA

Comparison with theory has been made with respect to two data sets. One set was from ECBC's 5-cm wind tunnels, and a second set was from the Czech Republic's 10-cm tunnel. In both cases, the data are for HD sessile drops on a glass substrate. Consistent with theory, the sessile drops are assumed to be segments of a sphere in shape; however, the experiments are deficient in not including either the contact angle or the height to diameter ratio as one of the independent variables. Thus, the comparison is not with a predictive theory, but involves the determination of the contact angle and m that results in qualitative agreement.

In both data sets, the primary measurements are initial droplet mass and downstream concentration of HD as a function of time. The mass of the droplet remaining is deduced from these data. In most cases, the errors in the technique results in unaccounted for mass or in some cases more mass than in the original drop. This error can be "corrected for" in most of mass remaining distributions; but, the correction is questionable at the end of the run. That is, at the end of the run, the concentration is lowest and of uncertain accuracy.

The table lists the test conditions for the cases considered here. In general, the quality of the theoretical fit to the experimental data is good as can be seen in Figures 7 and 8.

Table. Summary of Test Conditions from Czech Republic and ECBC

CZECH REPUBLIC DATA									ECBC DATA		
TEST	CR1	CR2	CR3	CR4	CR5	CR6	CR7	CR8	ECBC1	ECBC2	ECBC 3
NOMINAL CONDITIONS											
Q, μL	1	1	1	1	6	6	6	9	1	6	6
Wind Speed, m/s	1.77	0.26	0.26	0.26	1.77	1.77	1.77	1.77	0.22	1.61	1.61
TEST CONDITIONS											
Droplet Mass, mg	1.180	1.184	1.192	1.204	7.244	7.022	7.304	12.033	7.80	7.41	6.87
Droplet Volume, mm^3	0.938	0.940	0.947	0.957	5.75	5.58	5.80	9.56	6.28	5.89	5.46
Friction Velocity* m/s	0.096	0.04	0.04	0.04	0.096	0.096	0.096	0.096	0.04	0.096	0.096
Temperature, °C	35	35	35	35	35	35	35	35	50	35	35
CALCULATED PROPERTIES											
Contact Angle, β Deg	18	29	23	23	18	15	18	15	35	15	30
m	5	5	3	5	7	10	10	7	5	7	7
Initial Shape Factor,η_i	0.079	0.129	0.102	0.102	0.079	0.079	0.084	0.079	0.158	0.066	0.134
Time Factor, τ, hr	21.0	30.1	33.8	33.9	47.1	46.4	46.1	59.0	21.1	51.7	36.1

*Based on the 5-cm tunnel results, and the Czech Republic nominal wind speeds

The values of m and β were selected by trial and error with only visual appearance for criteria on which to base the goodness of the agreement. Thus, a mean value of m of say 7 would have produced relatively little change in the graphical results.

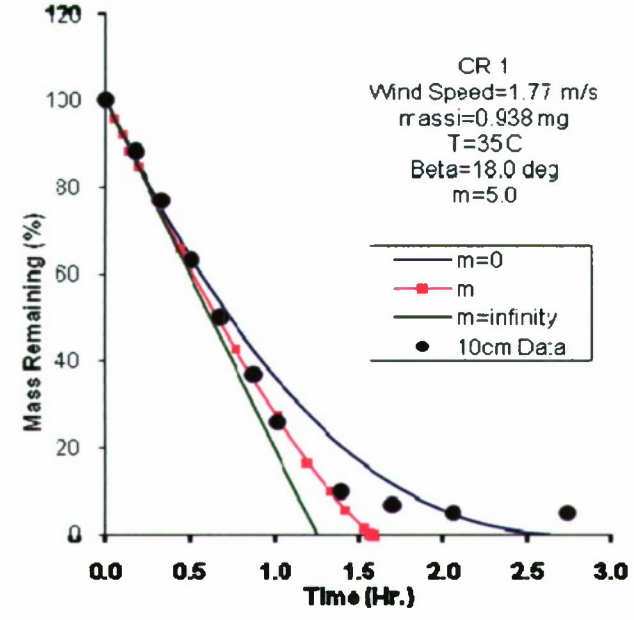

(1)

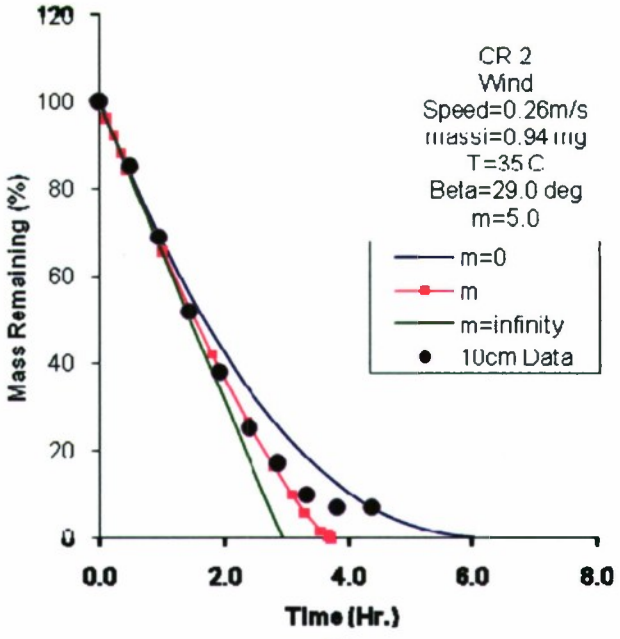

(2)

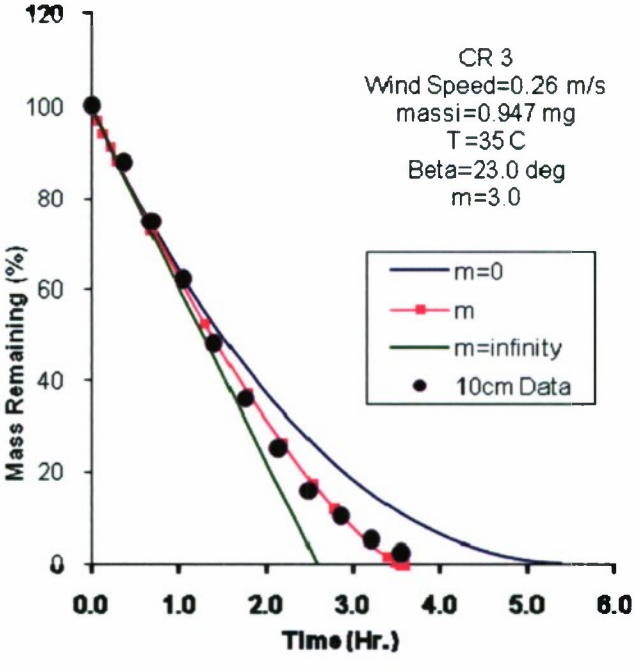

(3)

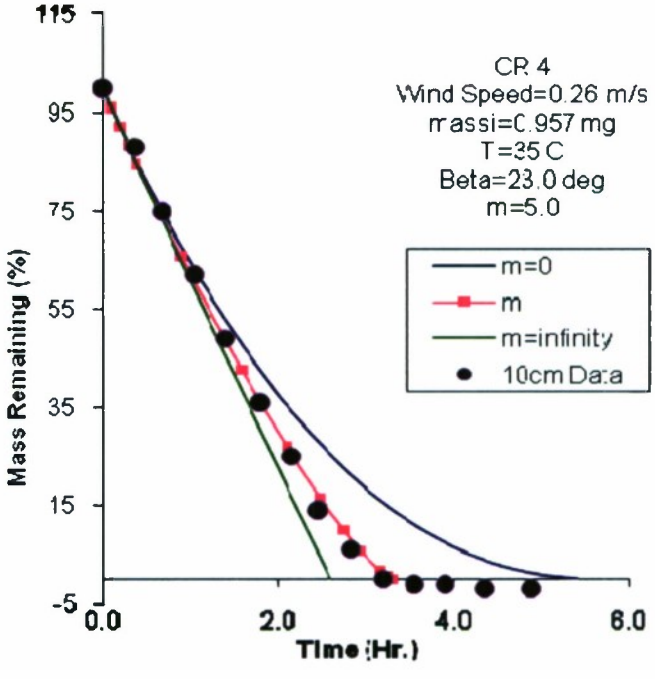

(4)

Figure 7. Comparison of Theoretical and Czech Experimental Mass Remaining

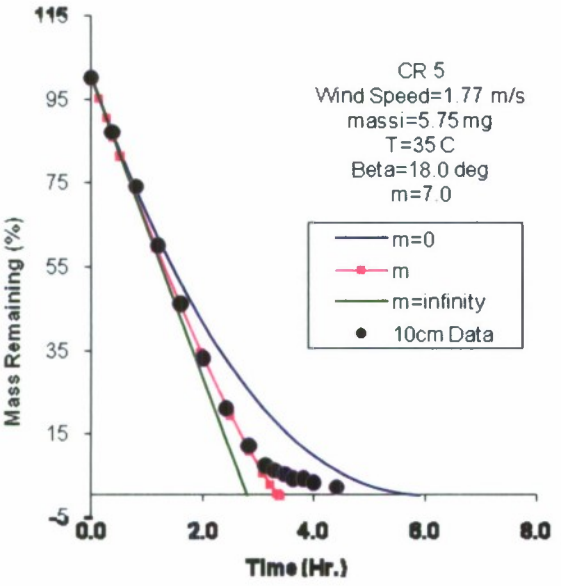

(5)

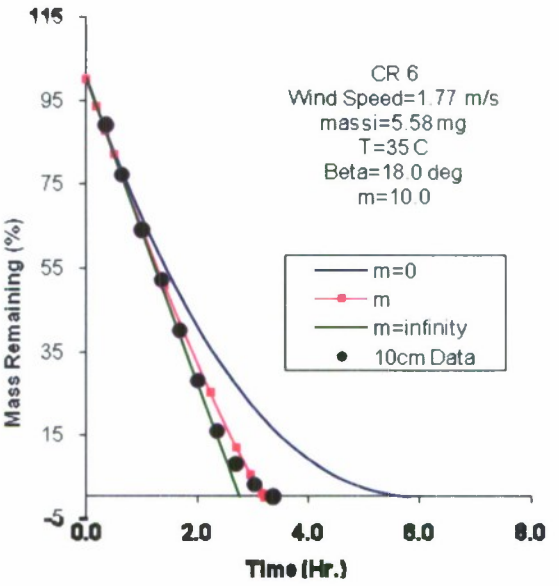

(6)

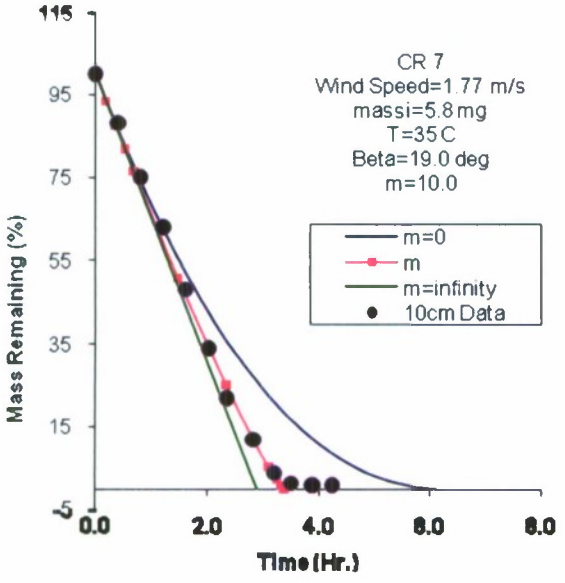

(7)

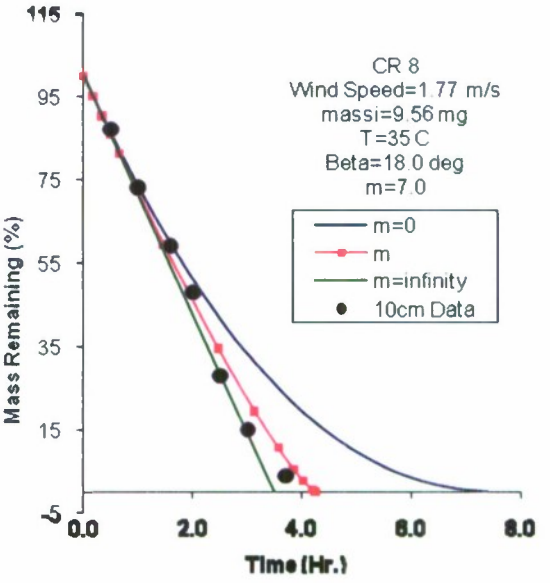

(8)

Figure 7. Comparison of Theoretical and Czech Experimental Mass Remaining (Continued)

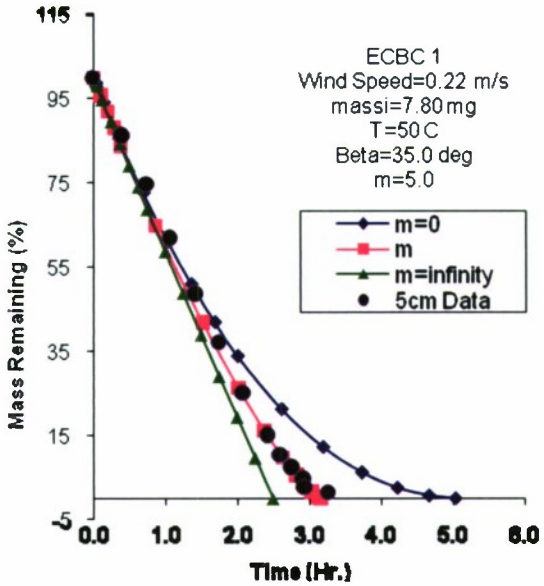

(1)

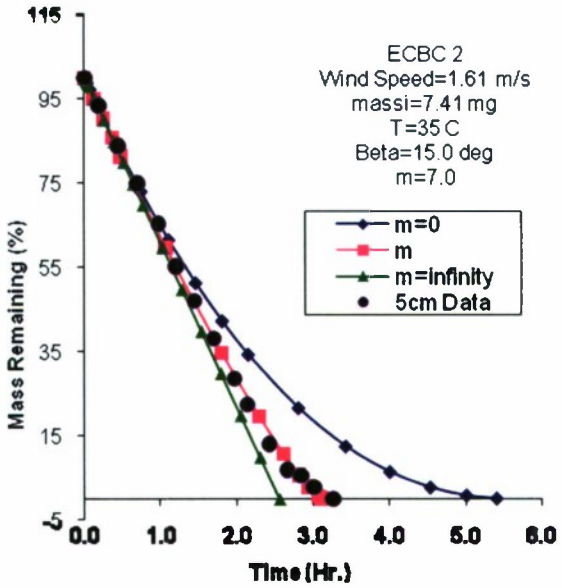

(2)

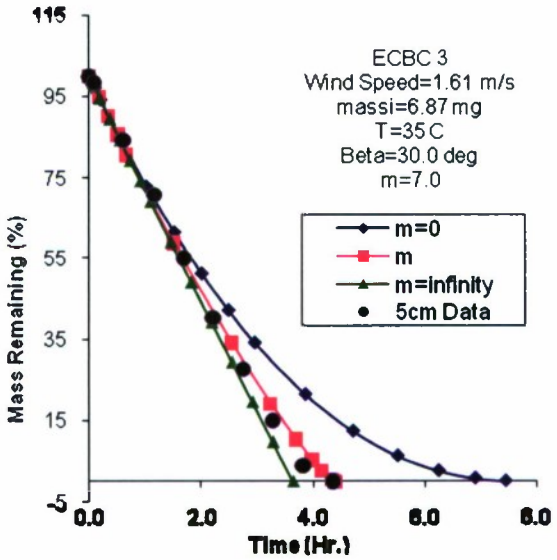

(3)

Figure 8. Comparison of Theoretical and ECBC Mass Remaining

The contact angle has a more sensitive effect. As already pointed out, computations using a constant value of 23.6°, which was the result from initial observations of three different sized drops, could not predict the total evaporation time within the constant diameter-constant shape factor limits. Therefore, predicting the contact angle is critical to accurate prediction of the evaporation history. The tabulated data provide limited information on the factors that effect β.

Six runs contain three drop size (initial mass or volume) conditions with all other conditions the same. These runs have a constant contact angle, β = 16.5° ± 1.5°, except for ECBC-3 which is considerably higher. Temperature variation is represented by three 35 °C runs of 1 μL drops and one run at 50 °C of a 6 μL drop. The 50 °C point suggests β increases with temperature. The effect of increasing wind speed decreases β from 23° to 15-18°. However, in conclusion, these 11 runs are insufficient to reliably determine trends in contact angle and exponent m.

Generalized Mass Remaining Distribution

The basic equation defining the mass-remaining distribution was specified in eq 1, which is repeated here.

$$\frac{d(\rho_{HD}\forall)}{dt} = -\dot{M} \tag{1}$$

A simple approximation is to take ρ_{HD} and $\dot{M}$ as constants at their initial values so that the mass or volume remaining becomes linear in time. Thus, the percent mass or volume remaining can be written.

$$\frac{M}{M_i} = 100 - 100\frac{t}{\tau} \tag{20}$$

Note that the definition of $\forall_i = \frac{\pi}{6} d_i^3 \left[\frac{3}{4}\eta_i + \eta_i^3 \right]$ in τ is slightly different from that of eq 10 in the inclusion of a term involving the shape factor. The time factor tabulated in the table corresponds to that of eq 10.

This suggests that a more general way of plotting the experimental data is $\frac{M}{M_i}$ versus $\frac{t}{\tau}$ where the linear part of the each curve should now coincide to the extent that τ is correctly determined. Figure 9 shows the results of plotting all 11 experimental distributions covering a range of conditions. The data are correlated well over the whole range. Good agreement should be expected here because the value of contact angle and thus the shape factor have been selected to give good agreement with the individual runs. Some of the data scatter at

large times is due to the measurement inaccuracy at very low concentration levels. The fact that, in some cases, the total droplet mass has not been accounted for confirms this conclusion.

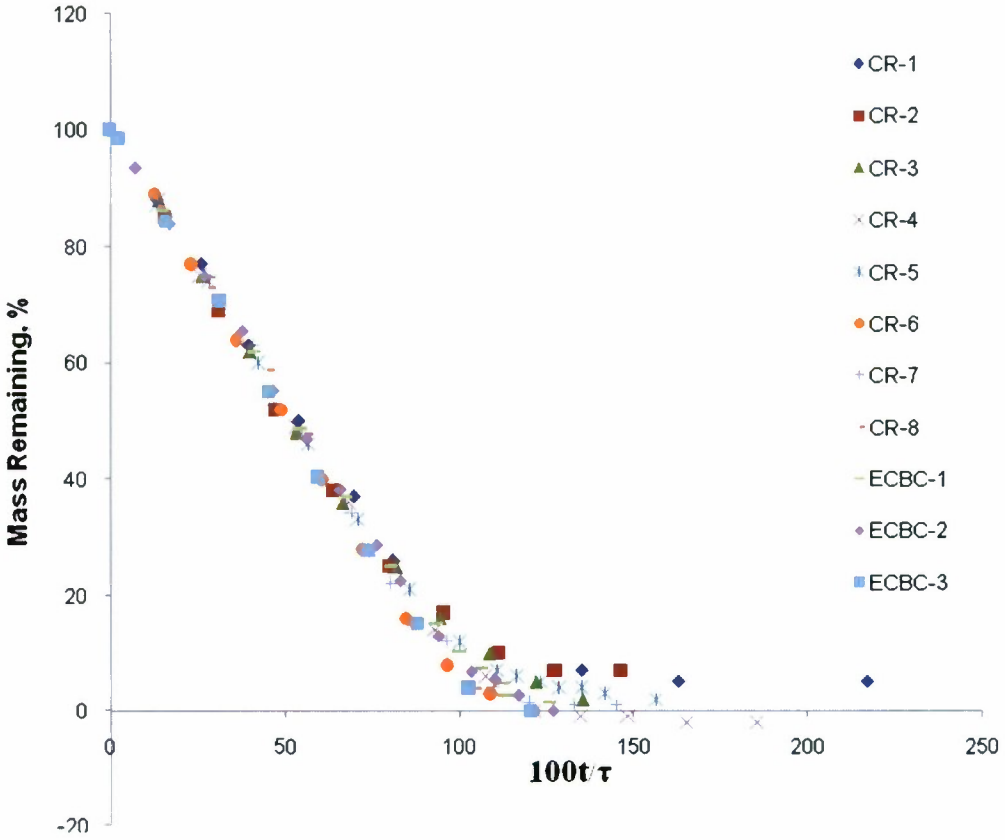

Figure 9. Correlation of the Experimental Data with τ

5. UNSTEADINESS

In analyzing field test data, the additional problem of varying atmospheric conditions needs to be addressed. The two most important are temperature and "wind velocity". The measurements indicate both of these quantities have short-term variations in minutes and longer-term average variations in hours. A characteristic response time of the evaporation of millimeter sized droplets might be characterized by d^2/ν, which for a 5.2 mm drop at 35 °C is 1.6 s. Multiplying by the Sc number gives $d^2/D = 4.2$ s. Presumably, the evaporation mechanism cannot respond to fluctuation faster than approximately 5 s. A time factor of 1.6 times the Prandlt number might describe the thermal response. If this analysis is correct, the evaporation responds even to the short-term (minutes) variation in conditions.

The way variable conditions affect the mass-remaining time-history can be described as follows: We start by calculating the mass loss as if the temperature and friction velocity remained constant at their initial values. The result of the calculation is $\rho_{HD}\forall = M$ versus a computed time $\bar{t}$ that can be related to the physical time. Because u_τ and all the thermodynamic properties that are functions of temperature are grouped in the evaporation rate term $\dot{M}/\rho_{HD}$ as in eq 3, the real time, t, is related to this transformed time by

$$\bar{t} = \int_0^t \frac{f(T(t))}{f(T_i)}\left[\frac{u_\tau(t)}{u_{\tau i}}\right]^{2/3} dt \qquad (21)$$

The subscript i refers to the initial conditions, and $f(T) = \left(\frac{D}{\nu^2}\right)^{2/3}\frac{c_w \nu}{\rho_{HD}}$ (see right hand side of eq 8) where the physical properties are functions of temperature; thus, f(T) defines the temperature dependency of the evaporation rate. By this procedure, we have grouped the sources of unsteady effects into a transformed time and separated its calculation from that of the mass as a function of transformed time.

5.1 Temperature Dependency

The evaporation rate's dependency on temperature has been discussed in a recent memorandum,[6] which came to the conclusion that the dependency is (where T is in °K)[†]

$$\dot{M} = \dot{M}_{ref\,@\,35C}\left[\frac{T - 91.6}{153}\right]^{17.2} \qquad (22)$$

which can be used in eq 21 in the form (where now T is in °C)

$$\frac{f(T(t))}{f(T_i)} = \left[\frac{T(t)+181.5}{T_i+181.5}\right]^{17.2} \qquad (23)$$

This relation is highly non-linear; therefore, even the nearly sinusoidal short-term variations in temperature could have a cumulative effect on the transformed time-real time relationship if the magnitude of the temperature variation is sufficiently large. However, as a first step, consider the longer-term unsteadiness or trends in speed and temperature.

5.2 Long-Term Unsteadiness in Speed

An increasing or decreasing trend in the wind velocity and temperature during the evaporation, which can be handled by the transformed time calculation, may exist in field tests. As a simple example, consider a hypothetical case where the "wind" speed increases linearly

[†] Note that $1/\rho_{HD}$ could also be included; however, it is not because it is such a weak function of temperature.

from the speed corresponding to a 0.096 m/s friction velocity to a speed that doubles the friction speed over a period of 3 hr (assuming constant temperature).

$$u_\tau = 0.096(1 + 1.0t/3.0) \tag{24}$$

The transformed time becomes

$$\bar{t} = \int (1 + 1.0t/3.0)^{2/3}\, dt \tag{25}$$

Using a simple transformation, $\xi = (1 + t/3.0)$, eq 25 can be integrated as

$$\bar{t} = 3\int_0^t \xi^{2/3} d\xi = \frac{9}{5}\xi^{5/3}\Big|_0^t = \frac{9}{5}\left[(1 + t/3)^{5/3} - 1\right] \tag{26}$$

Thus, for this simple example, we have an exact relationship between $\bar{t}$ and the physical time, and eq 26 can be solved for t as a function of $\bar{t}$.

$$t = 3\left[(1 + 5\bar{t}/9)^{3/5} - 1\right] \tag{27}$$

In the data from an actual field test, it will be very unusual to describe the actual velocity distribution analytically. Thus, in designing a FORTRAN program to perform the long-term analysis, provision has been made to input data points describing the measured time, temperature and speed trends. These data are used to calculate a table of transformed time versus physical time by simply averaging the integrand of eq 21 between successive points and multiplying by the time step and summing. To find the physical time corresponding to the transformed time, computed in the primary calculation of the volume, a table look-up and linear interpolation has been used.

Figure 10 also shows this result, which conforms to what is expected in that an increase in friction velocity implies an increase in evaporative mass flow; therefore, the time to achieve any given level of remaining mass must decrease. This figure also shows a comparison between the "exact" result using eq 27 and the result of taking 19 points in physical time versus speed as input and doing the approximate look-up and interpolation calculation. There is no discernable difference in the two techniques in this case.

5.3 Long-Term Unsteadiness in Speed and Temperature

Longer-term variation such as a decrease of the mean temperature of 6-8 °C over several hours produces a significant effect (see bottom panel in Figure 5 of reference 1.) As a model of this long-term temperature variation, assume a decrease of about 7 °C over a 4 hr period. For purposes of illustrating the significance of such a trend, the standard 35 °C reference

case is modified by this decrease in temperature and the linear increase in velocity previously considered. Equation 23 provides the temperature effect on the evaporation function required, and the temperature versus physical time input is

$$T = 35 - 7t/4 \tag{28}$$

with t in hours. Equations 24, 28, and 23 were used in eq 21 to calculate a table of $\bar{t}$ versus t values for the combined effect. The look-up physical time is plotted in Figure 10, which shows that the decrease in temperature approximately compensates for the increase in velocity.

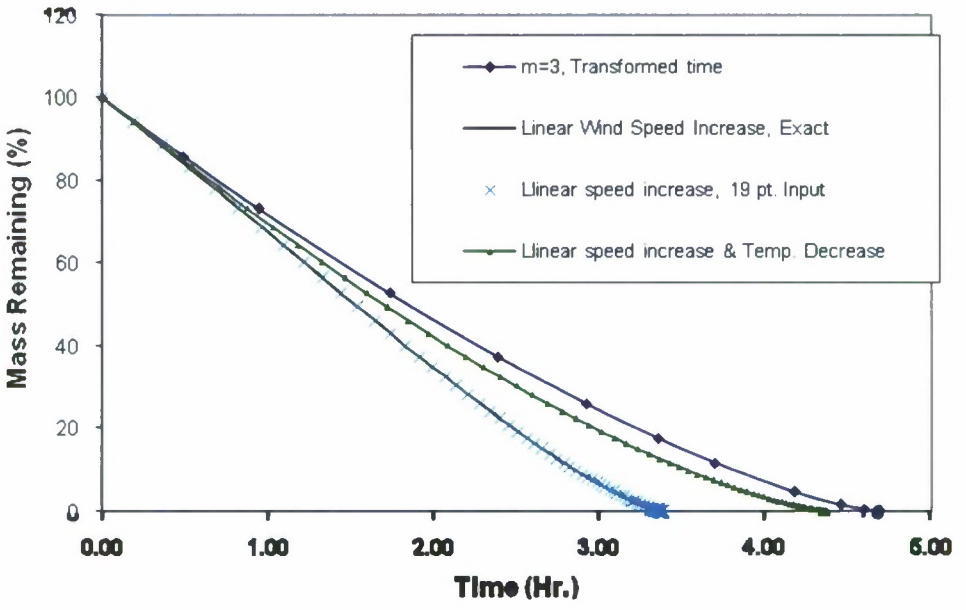

Figure 10. Effect of Long-Term Trends in Wind Speed and Temperature

5.4 Unsteady Short-Term Wind Speed Effects

Figure 11 provides an example of the wind speed data obtained from field tests[7] performed in the Czech Republic in 2002. Over an approximate 4 hr test, the average speed is about 0.2 m/s; the maximum speed is about 1 m/s; and the minimum speed is about 0 m/s.

Example of Velocity Measurements
HD on Glass
0.018 m (1.8 cm/0.7 in.) Height Above Ground

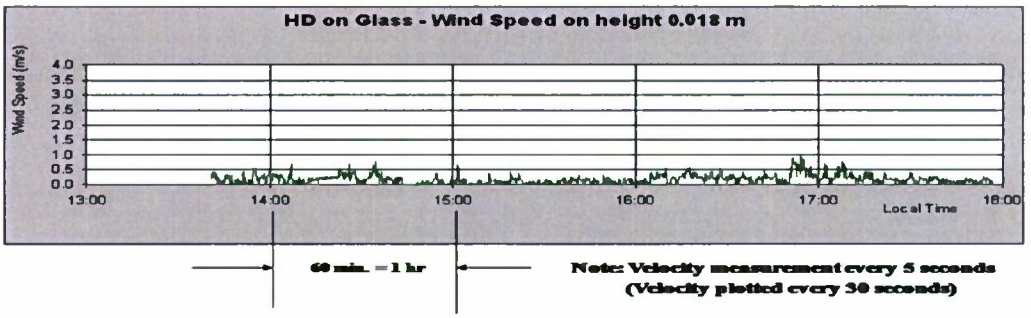

Figure 11. Example of Short-Term Wind Speed Field Test Data

These short-term oscillations (minutes) in wind speed can produce some effects as well as longer period (hours) changes. A simplified model is to assume the variation to be sinusoidal, which is a reasonable approximation to the speed distribution shown in Figure 12.

Measured Wind Speed Over a 4 Minute Interval
Outdoor Tests - HD on Glass
14:00 - 0.018 m/1.8 cm/0.7 in. Height

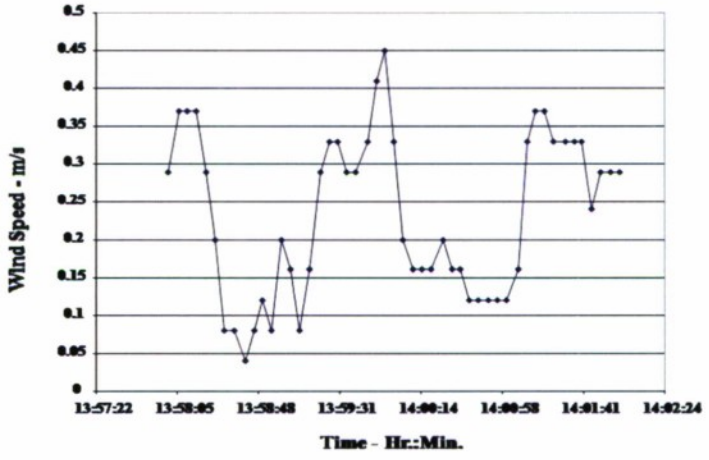

Figure 12. Wind Speed Variation over a 4 min Interval

If we assume that the friction velocity varies in proportion to a sine wave, we can write the transformed time as

$$\bar{t} = \int_0^t \left[\frac{0.096(1 + \sin(2\pi t / t_p))}{0.096} \right]^{2/3} dt \qquad (29)$$

We have taken the short-term oscillation period equal to 3 min for a full cycle. Thus, we are numerically integrating over a 180 s cycle, and the non-linearity in eq 29 results in a transformed time of 165.6 s or 92.0% of physical time. This means that over a 3 hr predicted evaporation time (transformed time), the end value in physical time $t = \bar{t}/0.92$ or 3.26 hr. Figure 13 illustrates this by taking the m = 3 solution at constant friction velocity and assuming the effect of the oscillations as specified by eq 29. The extent of the calculation has been limited to the initial 1000 steps of 10 s to resolve the short-term oscillation. The calculation of mass remaining versus the physical time plotted in Figure 13 and the scale of the plot is too coarse to observe the oscillations in the mass remaining.

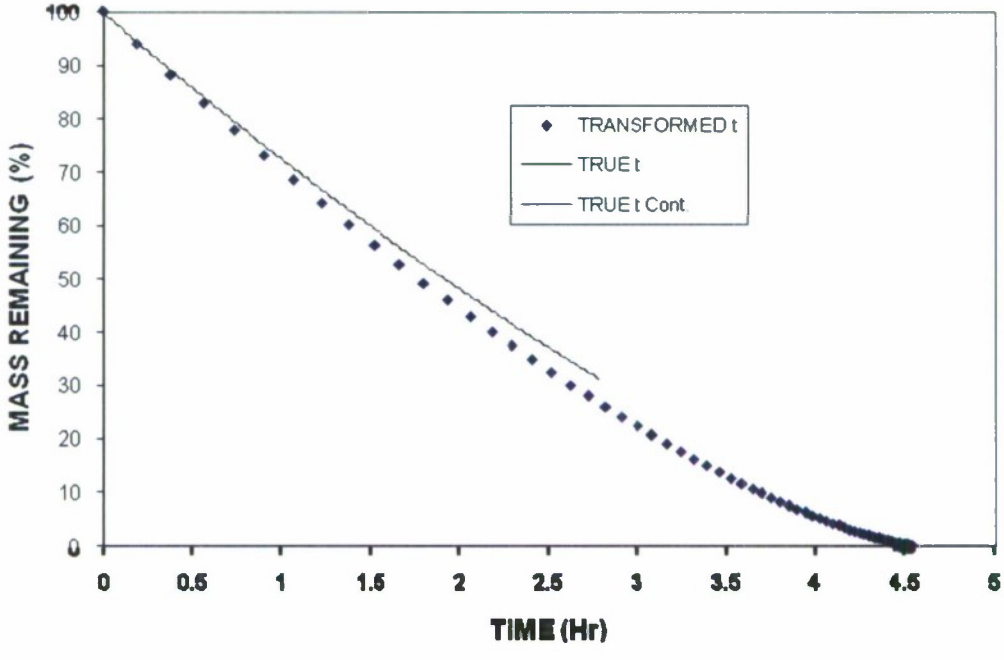

Figure 13. Effect of 3 min Sinusoidal Oscillation on Mass Remaining vs. Time

Figure 14 shows the final 63 steps of the Figure 13 true time curve at a very much expanded scale where the oscillation in the curve become clear. Three and a half cycles are shown here.

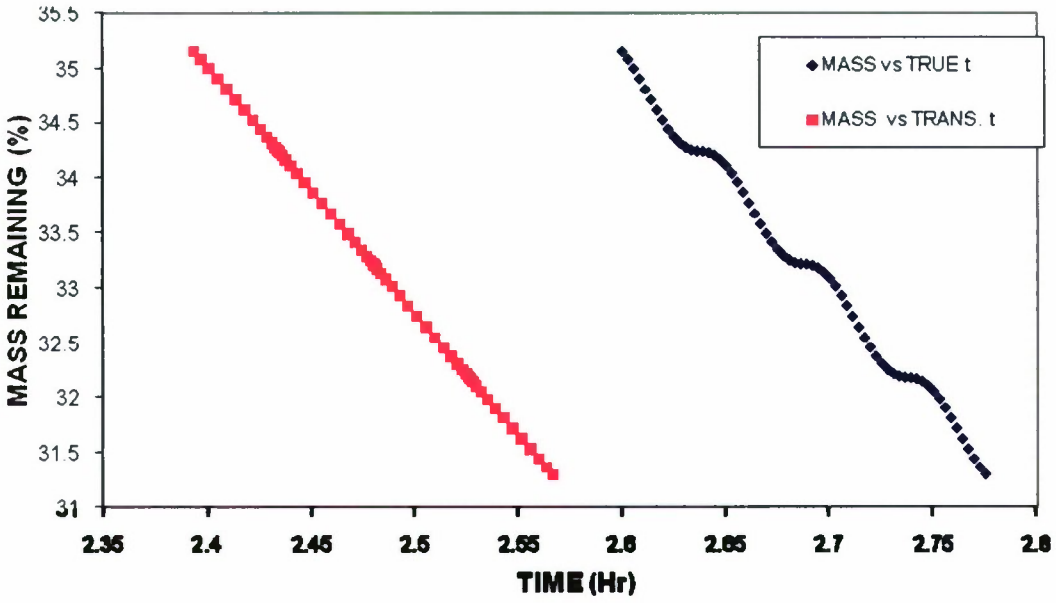

Figure 14. Mass Remaining vs. Time Expanded Scale

The assumed sinusoidal variation of the friction velocity is probably more server than might be expected in practice. Thus, the primary conclusions to be drawn from the above analysis of the short-term wind speed fluctuations is that the expected effect is, at most, an extension of 8% in the evaporation time.

5.5 Unsteady Short-Term Temperature Effects

As was pointed out earlier, eq 23 is highly non-linear, and the effects of the long-term variation in temperature are significant. However, an amplitude of only a few degrees in the short term oscillation is not enough. For example if $T_i = 35$ °C, and $T = 35 + \Delta T$, then

$$\frac{f(T(t))}{f(T_i)} = \left[\frac{216.5 + \Delta T}{216.5}\right]^{17.2} = \left[1 + \frac{\Delta T}{216.5}\right]^{17.2} \approx \left[1 + 17.2\frac{\Delta T}{216.5}\right] \qquad (30)$$

Thus, if the temperature oscillations are about ± 1 °C with a period of 1-3 min, the temperature factor changes only about ± 7% per °C. But more important, if the last term in eq 30 is valid, and these short-term oscillations are generally periodic, the oscillations will cancel over time and leave the mean of the mass-time curve unchanged. This does not mean that the oscillations would not be observable with appropriate instrumentation; however, they would appear as temperature waves superimposed on the steady-state trend.

6. CONCLUSIONS

An attempt has been made to present a rigorous determination of the mass remaining as a function of time. The basic idea behind the calculation is initially described for the case of a droplet segment of spherical geometry with constant base diameter. The segment is then characterized by the variation of the droplet shape factor (height/base diameter) or contact angle. It is pointed out that this is a limiting case.

A suggestion is advanced for the combined variation of diameter and shape factor (η) case where the shape factor is assumed as a power law function of the diameter.

$$\eta \propto d^m$$

The variation of m between its limiting conditions of $m = 0$ (constant shape factor) and $m \rightarrow \infty$ (constant base diameter) define a range of intermediate conditions.

Experimental data are needed to determine a suitable value of the exponent m.

Comparison of experimental data and analysis indicates the need to determine the initial shape factor (contact angle) accurately. By appropriately choosing the combination of shape factor and exponent m, good agreement between the analysis and experimental data can be obtained. More experimental data on the shape factor are needed to determine its dependence on the variables of the problem (temperature, drop size, etc.).

Introduction of a time factor, dependent on the conditions of the experiment, provides an effective method of correlating all the experimental data.

The question of unsteady atmospheric temperature and "wind" conditions has been addressed by introducing a transformed time. This time allows the mass remaining to be calculated as a function of a transformed time based on initial conditions. Then, the relationship between the transformed time and physical time is computed from the unsteadiness.

Blank

NOMENCLATURE

A	Surface area of evaporating drop
C	Proportionality constant in the Sherwood number equation
c_w	Concentration of vapor at the surface of drop
d	Diameter of sessile drop
D	Diffusivity of vapor in air
$F(T)$	Evaporation rate dependency on temperature
h	Height of sessile droplet
L	Characteristic length
M	Droplet mass
$\dot{M}$	Total evaporation rate
m	Exponent in relationship between shape factor and diameter
n	Number of data points
N	Evaporation rate per unit area
Q	Volume of drop
Re_d	Drop Reynolds number = $(u_\tau\, d)/\nu$
Sc	Schmidt Number = ν/D
$\overline{Sh_d}$	Average Sherwood Number = $\dot{M}\, d/A\, c_w\, D$
T	Temperature
t	Time
t_p	Oscillation time period
$\bar{t}$	Transformed time
u_τ	Friction velocity = $\sqrt{\nu\left(\frac{\partial u}{\partial y}\right)_w}$
$\forall$	Volume of surface drop

Greek Symbols

β	Contact angle of sessile drop
η	Droplet shape factor = h/d
σ	Non-dimensional time = t/τ
ν	Air kinematic viscosity
ξ	Transformation variable
ρ	Air density
ρ_{LD}	Density of liquid Agent
τ	Time parameter = $\frac{M_i}{\dot{M}_i}$
φ	non-dimensional diameter = d/d_i

Blank

LITERATURE CITED

1. Navez, H.K.; Chan, E.; Kehtarnavaz, N. *A Comprehensive Study of HD Sessile Droplet Evaporation on Impermeable, Non-Reacting Substrates*, Kettering University: Flint, MI, 2006.

2. Danberg, J.E. *Evaluation of 5-cm Agent Fate Wind Tunnels Velocity Profiles*; ECBC-CR-091; U.S. Army Edgewood Chemical Biological Center: Aberdeen Proving Ground, MD, 2007; UNCLASSIFIED Report (AD-A472 909).

3. Danberg, J.E. *Evaporation into Couette Flow;* ECBC-CR-092; U.S. Army Edgewood Chemical Biological Center: Aberdeen Proving Ground, MD, 2008; UNCLASSIFIED Report (AD-A477 975).

4. Baines, W.D.; James, D.F. Evaporation of a Droplet on a Surface. *Ind. Eng. Chem. Res.* **1994**, *33*, 411-415.

5. Weber, D.J.; Miller, M.C.; Shuely, W.J. Procedure to Adjust Wind Tunnel Data for Mass Recovery Efficiency. In *Proceedings of the Scientific Conference on Chemical & Biological Defense Research*, 13-15 November 2007; Battelle CBRNIAC Report SOAR-08-24; U.S. Army Edgewood Chemical Biological Center: Aberdeen Proving Ground, MD, 2008.

6. Danberg, J.E., January 8, 2007, *subject: Evaporation Rate Dependency on Temperature*, Memorandum to U.S. Army RDECOM/ECBC/T. Donnelly.

7. Weber, D.J.; Miller, M.C.; Shuely, W.J. Comparison of Agent Fate Wind Tunnel Velocity Profiles with Outdoor Wind Profile. In *Proceedings of the Scientific Conference on Chemical & Biological Defense Research*, 13-15 November 2007; Battelle CBRNIAC Report SOAR-08-24; U.S. Army Edgewood Chemical Biological Center: Aberdeen Proving Ground, MD, 2008.